International Journal of Pharmaceutical Research and Applications
Volume 10, Issue 2 Mar–Apr 2025, pp: 1358-1380 www.ijprajournal.com ISSN: 2456-4494

Formulation and Characterization of Voriconazole Nanostructured Lipid Carriers for Occular Drug Delivery

[1]Rajeshwari M K, [2]Sivaranjani J, [3]Kaviya K
K S Rangasamy college of Pharmacy, K S R Kalvi Nagar, Thiruchengode
K S Rangasamy college of Pharmacy, K S R Kalvi Nagar, Thiruchengode
K S Rangasamy college of Pharmacy, K S R Kalvi Nagar, Thiruchengode

Date of Submission: 01-04-2025 Date of Acceptance: 10-04-2025

ABSTRACT
Topical administration of ophthalmic drugs faces significant challenges, primarily associated with inadequate permeability and limited residence time in the eye. In an effort to overcome these issues, a formulation incorporating innovative lipidic nanoparticles with a specialized surface coating was developed. The nanoparticles, composed of Voriconazole-loaded Nanostructured Lipid Carriers (NLC), were prepared using a high-speed homogenization method. Stearic acid served as the solid lipid, Capmul MCM as the liquid lipid, and Poloxamer 188 as the surfactant. Central Composite design was employed to systematically vary the amount of solid lipid, the ratio of solid lipid to total lipid, and surfactant concentration, optimizing the NLC based on particle size, Polydispersity Index (PDI), and %Entrapment efficiency as dependent variables.The optimized Voriconazole-loaded NLC exhibited nano-sized particles with a uniform distribution and high %entrapment efficiency. These NLC were further enhanced by coating them with mucoadhesive chitosan hydrochloride solution. The formulated product underwent comprehensive characterization for various pharmaceutical parameters, including particle size, % EE, PDI, zeta potential, in vitro drug release behavior, morphology, ex vivo permeation, mucin interaction and stability. The surface-coated Nanostructured Lipid Carriers containing Voriconazole demonstrated a particle size of 114.16±7.919 nm, a PDI of 0.125±0.014, %Entrapment efficiency of 77.94±1.929%, and a positive zeta potential of +16.866±1.36 mV. This formulation exhibited sustained release, spherical morphology, non-irritant properties.

KEYWORDS: Voriconazole**,** Lipidic nanoparticles**,** Mucoadhesion**,** Chitosan hydrochloride**,** Poloxamer 188**, ,** In vitro drug release,Central Composite Design.

I. INTRODUCTION

(1)Over 285 million people worldwide, according to the World Health Organization (WHO), suffer from eye problems; this figure is projected to increase significantly over the next several decades.

(2)Infectious keratitis is an inflammation of the cornea produced by microbes. It is most related with bacteria, fungi or viruses that attack the corneal stroma, ensuing in inflammation and destruction of these structures resulting in visual impairment and blindness . Fungal keratitis (FK) is one of the most difficult to diagnose and treat . The occurrence of fungal keratitis depends upon the geographic location. It is more common in tropical and subtropical areas and relatively rare in temperate countries.

(3)The species that cause fungal keratitis commonly are Aspergillus, Bipolaris, Fusarium, Candida, and Curvularia with majority of cases caused by Candida, Fusarium and Aspergillus.

(4)One of the key mechanisms that fungi escape the immune response and establish infection is through the formation of biofilms. Fusarium, Candida, and Aspergillus clinical isolates have all been found to produce biofilms. A time dependent decline in efficacy with increase in minimum inhibitory concentration (MIC) is reported with commonly used antifungal agents such as amphotericin B, natamycin, itraconazole, terbinafine, fluconazole and voriconazole with the development of biofilm. This implies that the capacity to disrupt the biofilm can be advantageous in boosting antifungal potency.

(5,6) Fungal keratitis can be diagnosed based on distinctive clinical characteristics. The typical symptoms of keratitis include rapid onset of discomfort, photophobia, watering and discharge, and decreased vision. The basic sign of a fungal keratitis is a dry, elevated lesion with feathery or crenate margins and the development of satellite lesions. Symptoms are much milder than the signs in FK.Confocal microscopy, Laboratory analysis

International Journal of Pharmaceutical Research and Applications
Volume 10, Issue 2 Mar–Apr 2025, pp: 1358-1380 www.ijprajournal.com ISSN: 2456-4494

such as staining of tissue scrapings with Gram-stain, 10% potassium hydroxide (KOH) wet mount, lactophenol cotton blue, Giemsa, or calcofluor white, Polymerase chain reaction and Metagenomic deep sequencing can be employed for diagnostic purposes.

II. MATERIALS AND METHODS

Materials

Brinzolamide, Poloxamer 188, oleic acid, , glyceryl monostearate and chitosan were used of analytical grade.

Methods

(6) Hot melt emulsification technique coupled with high-speed homogenization was used to prepare NLCs. The lipids and the drug were heated together at a temperature 5^0 C above the melting point of the solid lipid, i.e. Stearic acid, at 75 ^{0} C. An aqueous phase comprising surfactant solution was heated at the same temperature. The lipidic phase was added dropwise in the aqueous phase under continuous stirring by a high-speed homogenizer (Heidolph (Inkarp), Germany). The temperature was kept constant throughout the process. After the completion of stirring, the dispersion was immediately brought to a temperature of 4-6 ^{0}C and stored at the temperature for 45 min so that the NLCs which were formed got stabilized in that state. The stirring speed and stirring time for the process was optimized using Poloxamer 1%w/v as a surfactant. For the selection of a suitable surfactant, four different surfactants viz. Tween 80, Poloxamer 407, Cremophor RH40, and Poloxamer 188 were screened.

International Journal of Pharmaceutical Research and Applications
Volume 10, Issue 2 Mar–Apr 2025, pp: 1358-1380 www.ijprajournal.com ISSN: 2456-4494

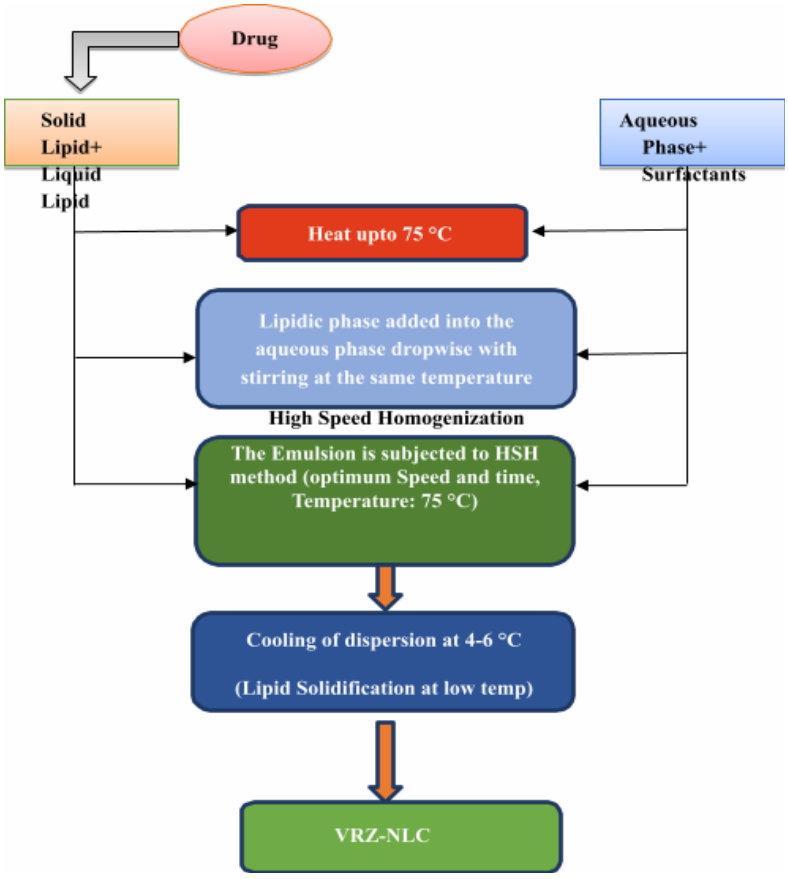

Schematic presentation of method of preparation of VRZ-NLC

Particle size, Particle size distribution and Zeta potential

(7,8)Particle size of NLC dispersion was determined using a Zetasizer (Nano ZS 90, Malvern Instruments Ltd., Malvern, UK) based on the dynamic light scattering phenomenon by illuminating the nanoparticles with a laser beam and examining the intensity variations in the scattered light, a technique known as dynamic light scattering (also known as photon correlation spectroscopy). The zeta potential reflects the electric charge on the particle surface and is an indicator of the physical stability of colloidal systems. It is measured by determining the electrophoretic mobility using the Malvern Zetasizer. The measurements were performed in double-distilled water.

% Drug Entrapment Efficiency (%EE) and %Drug loading(%DL)

(8,9)%Entrapment efficiency (EE) and %drug loading of NLCs were determined by measuring the concentration of free drug (unentrapped) in the external aqueous phase using the Protamine sulfate conjugation method for better aggregation of smaller particles giving accurate results. The NLC in dispersion were aggregated by adding 0.1 ml of 10 mg/ml Protamine sulfate solution overnight and centrifuged at 15000 rpm for 30 min at 15 °C to obtain a pellet. The supernatant was suitably diluted to determine the free drug. The % EE and %DL of the NLC were calculated by equation- 2 and equation-3, respectively.

$$\%EE = \{(Wtotal - Wfree)/Wtotal\} * 100 \text{ ----------(2)}$$

$$\%DL = \{(Wtotal - Wfree)/Wlipid\} * 100\text{----------(3)}$$

W_{total}, the total amount of drug used in the formulation; W_{free}, the analyzed amount of drug in the supernatant; W_{lipid} total amount of lipid in the formulation.

Transmission Electron Microscopy (TEM)

(9,10)The TEM was employed to determine the morphology and shape of the NLC dispersion. The samples were prepared by placing a

International Journal of Pharmaceutical Research and Applications
Volume 10, Issue 2 Mar–Apr 2025, pp: 1358-1380 www.ijprajournal.com ISSN: 2456-4494

5 µl droplet of the NLC dispersion onto a 300-mesh copper grid which is carbon-coated and allowing it to settle NLCs for 3–5 min. Afterwards, the excess fluid was removed, and the grid was dried carefully in the air.

In vitro drug release study

(11,12)In vitro drug release study was performed by Franz diffusion cell for a more realistic outcome as the volume of lachrymal fluid is less compared to other body fluids. Hence, the Franz diffusion cell provides better insights than the dialysis bag method. The study was performed by using a dialysis membrane (molecular weight cut off between 12,000 to 14,000 da, pore size 2.4 nm) attached in a diffusion cell between the donor and receptor compartments. 1 ml dispersion and 10 ml of simulated tear fluid (STF) pH 7.4 were kept in the donor compartment and the receptor compartment, respectively. The apparatuses were maintained at 32 ± 1^{0}C. At predetermined time intervals, 1 ml sample was withdrawn from the receptor compartment and immediately was replaced with the same amount of STF pH 7.4. The amounts of drug in the samples were analyzed. The drug release data was fitted into various mathematical models such as zero order model, first order model, Hixon Crowell model, Higuchi model and Korsemeyer-Peppas model to know the release kinetics of the formulation.

Preparation of Chitosan coated NLC:

(13,14) The final preparation of the drug entrapped surface coated lipidic nanoparticle formulation was achieved by coating the negatively charged lipidic nanoparticles with positively charged chitosan hydrochloride. A cationic Chitosan analogue was used in the aqueous phase of NLCs in order to prolong the corneal residence period and increase mucoadhesion to the cornea. For this purpose, appropriate amounts of the Chitosan hydrochloride were dissolved in water for 30 min in order to form a series of various concentrations (0.2%, 0.5% and 1%, w/v), then added dropwise in different ratio with drug loaded NLC dispersions under continuous stirring at 200 rpm for 20 mins. After that, the dispersion was assessed for zeta potential. Optimum concentration of the coating solution was selected based on results of zeta potential.

EVALUATION OF CHITOSAN COATED NLC

Particle size and Particle size distribution

(15,16) It is important to measure the particle size and particle size distribution after the surface coating. Particle size and particle size distribution was measured using the Zetasizer

%Entrapment efficiency and %Drug loading

(17,18)In order to confirm that coating process does not disrupt the nanoparticles or alter the matrix of the lipidic nanoparticles adversely, the %Entrapment efficiency and %drug loading was determined

Transmission electron microscopy:

(19,20)Along with zeta potential measurement, Transmission electron microscopy is confirmatory tool for to assess successful coating of Chitosan hydrochloride on the surface of NLC.

In vitro drug release study:

(21,22)To study the effect of the chitosan coating on the drug release behavior of the NLC and identify the mechanism and kinetics behind the release pattern, In vitro drug release study was performed by Franz diffusion cell using dialysis membrane (molecular weight cut off between 12,000 to 14,000 Da, pore size 2.4 nm). The drug release data was fitted into various mathematical models to know the release kinetics of the formulation

pH and isotonicity:

(23)The pH of the optimized surface coated lipidic nanoparticles was measured using calibrated pH meter at 25 ^{0} C. Maintaining isotonicity is a crucial attribute of the ophthalmic preparation to prevent tissue damage or irritation of cornea. Isotonicity of the formulation was evaluated by haemolytic method. A few drops of blood were mixed with the optimised formulation and examined at 450X under the microscope and compared with hypertonic, hypotonic, and regular saline solution.

Sterilization and Sterility testing

(24,25,26)The sterilization of the optimized formulation was carried out using membrane filtration technique. Optimized formulation was passed through membrane filters (0.22 µm) aseptically. Sterility testing was carried out as per IP 2010 by direct inoculation method. The samples were incubated for not less than 14 days in alternative fluid thioglycolate medium at 30-35 ^{0} C and Soyabean casein digest medium at 20-25 ^{0} C and checked for growth of microorganisms.

Stability studies:

International Journal of Pharmaceutical Research and Applications
Volume 10, Issue 2 Mar–Apr 2025, pp: 1358-1380 www.ijprajournal.com ISSN: 2456-4494

(27,28,29)The stability studies were performed to determine the physical stability of the prepared formulation under recommended temperature and relative humidity (RH) conditions to check the effects of storage conditions and effect of the presence of formulation components. The stability studies of the formulation were carried out under different storage conditions as per ICH guidelines, specifically 5 ± 3°C and 30 ± 2°C/60 ± 5% RH. The samples of stability studies were evaluated at 0, 0.5, 1, 2, 3, 4, 5 and 6 months for physical appearance, particle size, PDI and zeta potential. Each measurement was done in triplicate.

Optimization of VRZ-NLC:

The concept of DoE was used to optimize the formulation. 3 level-3 factor central composite design (CCD), originally developed by Box-Wilson, was selected for optimization of the response variables of Particle size (Y_1), Particle size distribution (Y_2), and %Entrapment efficiency (Y_3). The amount of total lipid (X_1), concentration of surfactant (X_2), and solid: total lipid ratio (X_3) were selected as independent variables. CCD is made up of factorial design, axial(star) points, and center points and can estimate the curvature and second-order response surface. (142)A 2^3 factorial design made the core of the experiment. The three variables were taken at two levels, high and low, which were coded as +1 and -1, respectively. Three replicates were performed at the center point, coded as 0, to estimate the experimental error. Six more runs called axial(star) points coded as ±α were performed to check the responses falling outside the design cube. The distance of the axial point from the center point was calculated by $\alpha=2^{n/4}$(n is the number of independent variables, here α=1.68). So, a total of 17 runs were performed in this study according to CCD (2^n+3+2n, n=number of independent variables, 3) Table shows three independent variables studied along with their corresponding levels and dependent variables. A total of 17 combinations of different levels of the three variables were performed The experimental design and statistical analysis were performed by using the Design Expert software® (Version 11, Stat-Ease Inc., Minneapolis, USA).

Independent and dependent variables for optimization of VRZ-NLC

Independent variables			
Coded value	Amount of total lipid(mg) X_1	Conc. of surfactant (%w/v) X_2	Solid: total lipid ratio X_3
-1.68	131.82	0.58	0.666

International Journal of Pharmaceutical Research and Applications
Volume 10, Issue 2 Mar–Apr 2025, pp: 1358-1380 www.ijprajournal.com ISSN: 2456-4494

-1	200	0.75	0.7
0	300	1.0	0.75
1	400	1.25	0.8
1.68	468.18	1.42	0.834
Dependent variables			
Y_1	Particle size (nm)		
Y_2	PDI		
Y_3	%Entrapment efficiency		

Design matrix for optimization of VRZ-NLC

Std	Run	Amount of lipid (mg) X_1	Concentration of stabilizer %w/v X_2	Solid: total lipid ratio X_3
13	13	300	1	0.66591
3	2	200	1.25	0.7
4	14	400	1.25	0.7
2	16	400	0.75	0.7
1	17	200	0.75	0.7
15	1	300	1	0.75
12	3	300	1.42045	0.75
10	6	468.179	1	0.75
17	7	300	1	0.75
11	9	300	0.579552	0.75
16	11	300	1	0.75
9	12	131.821	1	0.75
7	4	200	1.25	0.8
5	8	200	0.75	0.8
8	10	400	1.25	0.8
6	15	400	0.75	0.8
14	5	300	1	0.83409

III.

IV. RESULTS AND DISCUSSION:

Melting point of VRZ

Melting point of VRZ was determined by capillary melting point apparatus and it was found to be from 132 ^{0} C -135 ^{0} C. The reported melting point of VRZ is 134 ^{0} C.

Fourier transformed Infrared spectroscopy:

FTIR spectrum of VRZ recorded by FTIR spectrophotometer (Alpha model Bruker) is shown in figure. The characteristic IR peaks for respective functional groups present in the drug are summarized in Table. The recorded FTIR spectra was compared with reference spectrum and was found to be identical with reference spectrum.

International Journal of Pharmaceutical Research and Applications
Volume 10, Issue 2 Mar–Apr 2025, pp: 1358-1380 www.ijprajournal.com ISSN: 2456-4494

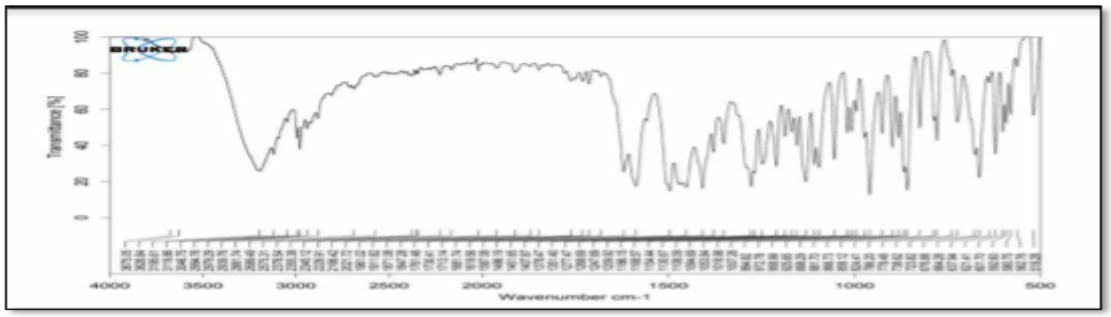

FTIR spectra of VRZ Table

Results of FTIR study

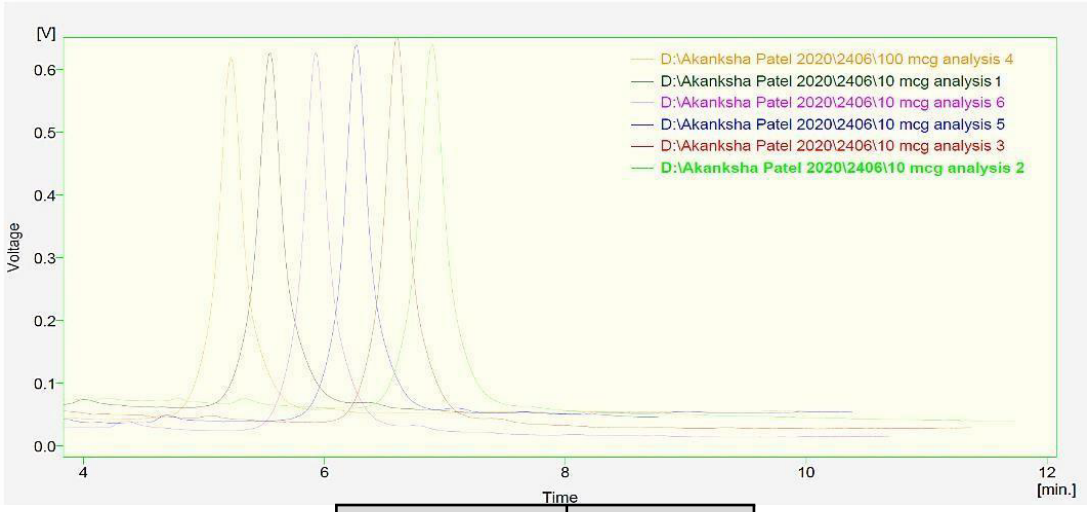

Peak cm^{-1}	Functional group
3195.61	-OH
1451	C-N stretch
1587	C-F stretch

Estimation of VRZ by HPLC method:

An HPLC instrument (Model LC 20AT, Shimadzu, Japan) was used to determine VRZ concentrations according to the method outlined in the literature [25],[26]. A volume of 20 µL of each sample was injected into the analytical column (Syncronis $C_{18,}$ 250 mm×4.6 mm, particle size 5µ, Thermofisher Scientific, USA). The mobile phase formed of a mixture of acetonitrile and water in the ratio of 60:40 (v/v), which was pumped at a flow rate of 1.0 mL/min at room temperature. The eluents were analysed spectrophotometrically at 256 nm. The retention time and theoretical plate were found to be 5.214±0.033 min and 2974.333±245.002 respectively (n=6). The system suitability data and overlay plot is shown in table 24 and figure 11 respectively. The system was found to be suitable for the method as %relative standard deviation for retention time was found to be 0.638 (%RSD<2), theoretical plates >2000 and asymmetry<2. (n=6)

International Journal of Pharmaceutical Research and Applications
Volume 10, Issue 2 Mar–Apr 2025, pp: 1358-1380 www.ijprajournal.com ISSN: 2456-4494

Results of system suitability

Sr. No	Retention time (Rt)min	Theoretical plate	Asymmetry
1	5.153	2485	1.043
2	5.230	3038	1.112
3	5.223	3123	1.157
4	5.237	3139	1.126
5	5.243	3054	1.125
6	5.203	3007	1.163

Linearity of analytical procedure is its ability (within a given range) to obtain test, which are directly proportional to area of analyte in the sample. The linearity data and overlay are shown in table and figure 12 respectively. The calibration plot was constructed using AUC and concentration (n=3). The regression equation and correlation co-efficient were found to be y = 11.766x - 8.2493 and 0.9977 respectively.

Overlay of system suitability

Results of linearity

Sr No.	Conc.(µg/ml)	Area (n=3, ±SD)
1	10	117.9093 ±1.734
2	20	223.29±4.936
3	30	336.2067±6.167
4	40	454.9873±8.696
5	50	590.63±8.727

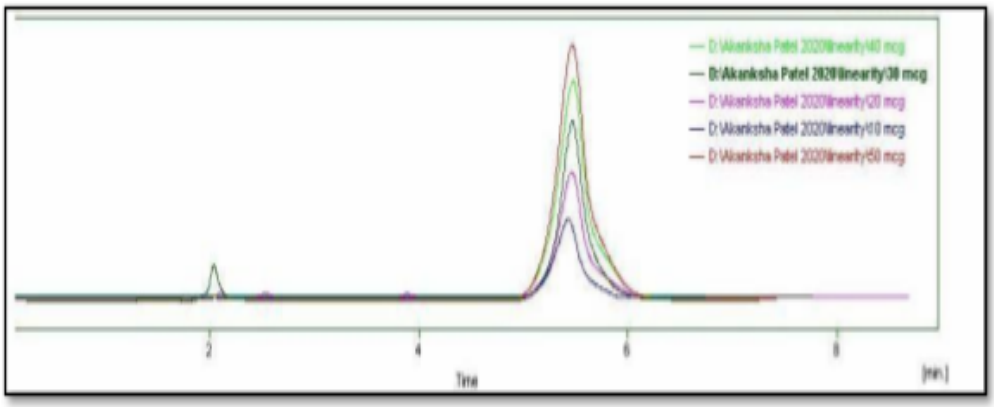

Overlay of linearity

Screening of components:

Incorporation of both solid and liquid is essential in the formulation of NLC. The lipids were selected based on their ability to solubilize drugs. If the drug does not have good solubility in lipids, it will not remain in lipidic particles and poor %EE will be seen. Further, the EE% of lipid nanoparticles can be improved by reducing the crystallinity of solid lipids. The liquid lipid decreases the crystallinity index of solid lipids in

International Journal of Pharmaceutical Research and Applications
Volume 10, Issue 2 Mar–Apr 2025, pp: 1358-1380 www.ijprajournal.com ISSN: 2456-4494

blends, and thus the crystallinity of lipid nanoparticles. In the solubility study, a cost-effective method of visual observation was used to detect insoluble VRZ crystals.

Screening of solid lipids:

The solubility of VRZ was studied in various solid lipids like Sterotex, Gelucire 43/01, Precirol ATO5, Compritol 888ATO and stearic acid which is summarised in figure. Stearic acid showed the highest solubility of VRZ followed by Sterotex and Compritol 888ATO. So Stearic acid was further selected for the formulation development of VRZ-NLC.

Screening of liquid lipids:

The solubility of VRZ was studied in different liquid lipids such as Capmul MCM, Captex 200P, Captex 355, Maisin CC and Labrafac PG is summarised in figure. Capmul MCM showed significantly higher solubility of VRZ which could be attributed to its chemical nature and inherent self-emulsifying property.

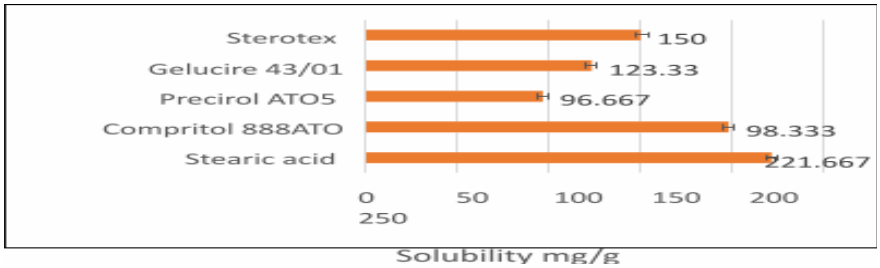

Data shown are of mean ± SD(n=3)
Solubility study of VRZ in solid lipid.

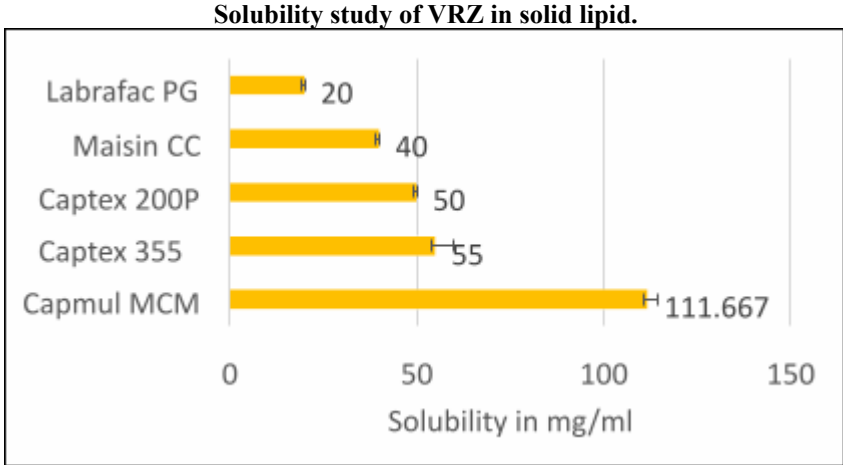

Data shown are of mean ± SD(n=3)
Solubility study of VRZ in liquid lipids

Miscibility of solid- liquid lipids:

International Journal of Pharmaceutical Research and Applications
Volume 10, Issue 2 Mar–Apr 2025, pp: 1358-1380 www.ijprajournal.com ISSN: 2456-4494

Miscibility of the two lipids is a principal factor in formulation of NLC. A higher ratio of liquid lipid in the mixture could be useful for a higher entrapment efficiency, however, at the same time the consistency of the solid lipid-liquid lipid mixture cannot be compromised because fluidic mixture of the lipids will not form a solid matrix. The selected solid and liquid lipids with the highest solubilizing ability i.e., Stearic acid and Capmul MCM respectively, were mixed in different ratios, viz., 90:10, 80:20, 70:30, 60:40, and 50:50 for evaluating phase compatibility of the solid lipid-liquid lipid mixture. The results of the smear test are summarised in table 26. 90: 10 solid to liquid lipid ratio was not selected for further studies as incorporation of very less amount of liquid lipid will not produce sufficiently imperfect NLC structure leading to poor entrapment efficiency and stability.

Screening of binary mixture of Solid Lipid (SL) & Liquid Lipid (LL)

Solid Lipid (SL)	Liquid Lipid (LL)	Ratio of SL: LL	Observation
Stearic acid	Capmul MCM	90:10	No oil spot is observed
		80:20	No oil spot is observed
		70:30	No oil spot is observed
		60:40	Oil spot is observed Slightly
		50:50	Oil spot is observed prominently

Optimization of process variables:

The stirring time and stirring speed of high-speed homogenizer (Heidolph(Inkarp), Germany) are critical process parameters which affect the CQAs such as particle size and particle size distribution. They were found to be of medium risk in FMEA. So, they were optimised using traditional trial and error approach. The optimisation of stirring speed and stirring time was carried out at three levels of stirring speed (5000, 7500 and 10000 rpm) and two levels of stirring time (10 and 20 minutes). The results of optimisation of process parameters are presented in Table . The stirring at 5000 rpm and 7500 rpm produced stable dispersions while stirring at 10000 rpm resulted into aggregation and phase separation. This might be attributed to higher shear force giving rise to smaller particles which do not have sufficient surfactant concentration to produce stable dispersions. The synergy between stirring speed and stirring time is essential as over stirring of the particles will impart charge on the particles due to hydrolysis of the liquid lipid and surfactant and under stirring will not provide enough coverage of the surfactant on the particle surface. Both will result into instability of the dispersion. Stirring at 5000 rpm for 20 min produced stable dispersion. Moreover, desired results were obtained at lower energy output (at 5000 rpm as compared to 7500 rpm). So, stirring speed of 5000 rpm and stirring time of 20 min were fixed for further experiments.

International Journal of Pharmaceutical Research and Applications
Volume 10, Issue 2 Mar–Apr 2025, pp: 1358-1380 www.ijprajournal.com ISSN: 2456-4494

Results of optimization of process parameters.

Sr No.	Stirring speed rpm	Stirring time(min)	stability
B25	5000	10	Phase separation
B21	**5000**	**20**	**stable**
B 26	7500	10	stable
B 27	7500	20	Phase separation
B 28	10000	10	Phase separation
B29	10000	20	aggregation

Screening of surfactants:

Four different surfactants viz. Tween 80, Poloxamer 407, Cremophor RH40, and Poloxamer 188 were investigated for preparing VRZ-NLC. Cremophor RH40 and Poloxamer 407 could not produce a dispersion of nanoparticles and the dispersion got aggregated immediately. Poloxamer 188 and Tween 80 produced NLC with particle size 26.59 nm and 95.49 nm, respectively. Poloxamer 188 could produce a stable dispersion while Tween 80 could not. This may be because Poloxamer 188 is a non-ionic linear copolymer with a large molecular weight compared to Tween 80. Hence, Poloxamer 188 provided an adequate barrier and repelled encroaching particles.

Drug Excipient Compatibility

FTIR spectra of pure Voriconazole and the physical mixtures of drug and selected excipients (VRZ+Stearic acid, VRZ+Capmul MCM, VRZ+Poloxamer 188) did not show any significant change in peaks of the drug, hence it was concluded that drug and excipients are compatible.

Optimization of the VRZ-NLC:

FMEA suggested that three factors viz, amount of lipid(mg), concentration of surfactant(%w/v), and solid: total lipid ratio played a crucial role in the preparation of VRZ-NLC. Hence, these variables were investigated by three-level three-factor centralcomposite design. The data displayed in table 28 obtained from the different batches was subjected to analysis in Design Expert 11 software. The generated mathematical model was statistically significant. ($p<0.05$). The obtained response surface plots and contour plots for the responses identified earlier were depicted in figure 15-21. In a contour plot, the response surface is viewed as a two-dimensional plane where all points that have the same response are connected to produce contour lines of constant response. A surface plot generally displays a three-dimensional view that may provide a clearer picture of the response. The mathematical model demonstrates the main effect and interaction effect between the same/ different variables. The co-efficient in the equations explain the magnitude and direction of the effect on the response. The quadratic model is best fitted for Y_1 and Y_2 while the linear model is the best fitted for Y_3.

International Journal of Pharmaceutical Research and Applications
Volume 10, Issue 2 Mar–Apr 2025, pp: 1358-1380 www.ijprajournal.com ISSN: 2456-4494

Design matrix of optimization of VRZ-NLC with responses

	Independent variables			Dependent variables (responses)		
Standard run	Amount of total lipid(mg) X_1	Conc. of surfactant (%w/v) X_2	Solid: total lipid ratio X_3	Particle size (nm) Y_1	PDI Y_2	%EE Y_3
1	200	0.75	0.7	127.32	0.293	72.29
2	400	0.75	0.7	37.23	0.232	79.13
3	200	1.25	0.7	143.12	0.475	69.01
4	400	1.25	0.7	35.21	0.147	75.15
5	200	0.75	0.8	73.19	0.124	72.93
6	400	0.75	0.8	47.54	0.21	80.58
7	200	1.25	0.8	100.23	0.39	70.12
8	400	1.25	0.8	46.24	0.224	76.56
9	131.821	1	0.75	157.43	0.43	67.28
10	468.179	1	0.75	31.65	0.194	79.01
11	300	0.579552	0.75	30.98	0.136	76.47
12	300	1.42045	0.75	47.46	0.235	71.01
13	300	1	0.66591	99.12	0.345	72.84
14	300	1	0.83409	48.03	0.235	73.87
15	300	1	0.75	42.39	0.133	75.89
16	300	1	0.75	48.33	0.101	76.96
17	300	1	0.75	52.34	0.09	75.47

Effect of formulation variables on Particle size (Y1)

ANOVA table of particle size

Source	Sum of Squares	df	Mean Square	F-value	p-value	
Model	26594.42	9	2954.94	67.66	< 0.0001	significant
X_1	17521.83	1	17521.83	401.17	< 0.0001	significant
X_2	331.02	1	331.02	7.58	0.0284	significant
X_3	1912.26	1	1912.26	43.78	0.0003	significant
X_1X_2	266.34	1	266.34	6.10	0.0429	significant
X_1X_3	1751.14	1	1751.14	40.09	0.0004	significant
X_2X_3	17.88	1	17.88	0.4094	0.5427	not
X_1^2	3597.44	1	3597.44	82.37	< 0.0001	significant
X_2^2	32.39	1	32.39	0.7415	0.4177	not
2 X_3	1231.40	1	1231.40	28.19	0.0011	significant
Residual	305.73	7	43.68			
Lack of Fit	255.61	5	51.12	2.04	0.3609	not
Pure Error	50.12	2	25.06			
Cor Total	26900.16	16				

Fit statistics			
$_R2$	Adjusted R^2	Predicted R^2	Adeq.
0.9886	0.9740	0.9230	27.7141

International Journal of Pharmaceutical Research and Applications
Volume 10, Issue 2 Mar–Apr 2025, pp: 1358-1380 www.ijprajournal.com ISSN: 2456-4494

The average particle size of different batches of VRZ- NLC varied from 30.98 nm to 157.4 nm as shown in Table 28. The effect of selected formulation variables on particle size (Y_1) is presented in Table 29 and the main effects X_1, X_2, X_3, and interaction effects X_1X_2, X_1X_3, X_1^2, X_3^2 are found to be statistically significant. Equation 8 representing the linear and quadratic interactions for response Y_1 is: $Y_1=+3484.010-3.418X_1+53.472X_2-7514.769X_3-0.2308X_1X_2+2.959X_1X_3+119.600X_2X_3+0.0017X^2-27.119X^2+4180.538X^2$ 8

Equation 8 shows the quantitative effect of all three variables (X_1, X_2, and X_3) and their linear and quadratic interactions on the response Y1. The main effects of X1, X2, and X3 represent the average result of changing 1 variable at a time, while the interaction terms (X_1X_2, X_1X_3, X_2X_3, X_1^2, X_2^2 and X_3^2) show how the particle size changes when two variables were changed simultaneously. An increase and decrease in response are represented by positive and negative signs, respectively.

The regression equation of response Y_1 shows that all three variables significantly affect the particle size. X_1 and X_3 affect particle size negatively while X_2 shows a positive effect. As soon as the lipidic phase is added to the aqueous phase, the shear force produced by the high-speed homogenizer reduces the particle size immediately, which is further stabilized by the surfactant by decreasing interfacial tension. Moreover, during stirring, surfactant molecules get adsorbed on the surface of lipidic particles and stabilize them. When there is enough amount of lipid and surfactant, a smaller size is obtained ,but if X_1 is decreased and X_2 is increased, it will lead to an increase in the viscosity of the external phase, formation of micelles and change in orientation of surfactant molecules, which will result in an increase in the particle size. This mathematical relationship between dependent variables and independent variables is depicted with the help of 3D response surface graphs and contour plots. The effect of X_1 and X_2 and their interaction when X_3 was kept at a fixed level (0.75) is shown in figure. Simultaneous increase in the concentrations of X_1 and X_2 demonstrated a negative effect on the particle size as seen in figure .

International Journal of Pharmaceutical Research and Applications
Volume 10, Issue 2 Mar–Apr 2025, pp: 1358-1380 www.ijprajournal.com ISSN: 2456-4494

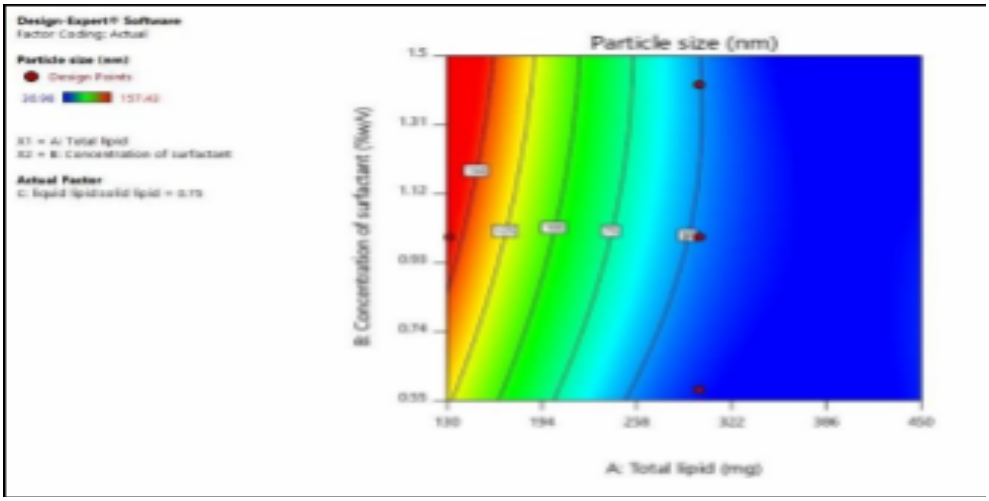

Contour plot of Particle size

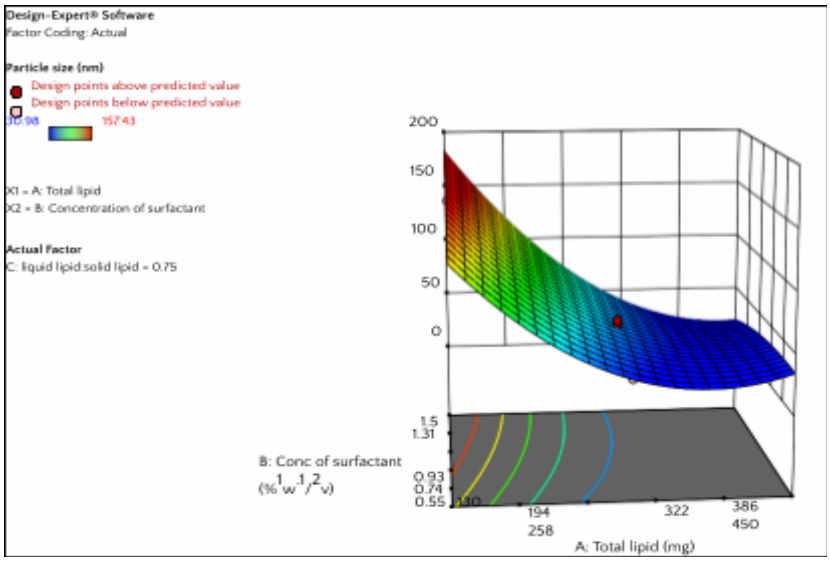

3D surface plot of Particle size

Effect of formulation variables on PDI (Y2)

The PDI of different batches of VRZ-NLC varied from 0.09 to 0.475 as shown in Table. The effect of selected formulation variables on PDI (Y_2) is presented in Table 30 and found to be statistically significant.

ANOVA table of PDI

Source	Sum of Squares	df	Mean Square	F-value	p-value	
Model	0.2138	9	0.0238	54.94	< 0.0001	significant
X_1	0.0549	1	0.0549	127.00	< 0.0001	significant
X_2	0.0216	1	0.0216	50.03	0.0002	significant

International Journal of Pharmaceutical Research and Applications
Volume 10, Issue 2 Mar–Apr 2025, pp: 1358-1380 www.ijprajournal.com ISSN: 2456-4494

X_3	0.0108	1	0.0108	24.98	0.0016	significant
X_1X_2	0.0337	1	0.0337	77.89	< 0.0001	significant
X_1X_3	0.0119	1	0.0119	27.61	0.0012	significant
X_2X_3	0.0042	1	0.0042	9.68	0.0170	significant
X_1^2	0.0551	1	0.0551	127.43	< 0.0001	significant
X_2^2	0.0071	1	0.0071	16.54	0.0048	significant
2 X_3	0.0435	1	0.0435	100.65	< 0.0001	significant
Residual	0.0030	7	0.0004			
Lack of Fit	0.0020	5	0.0004	0.8129	0.6323	not significant
Pure Error	0.0010	2	0.0005			
Cor Total	0.2168	16				
Fit statistics						
$_R2$	Adjusted R^2	Predicted R^2	Adeq. Precision			
0.9860	0.9681	0.9184	23.1495			

Equation 9 representing the linear and quadratic interactions for response Y_2 is:Y_2= 17.90425 -0.008027X_1 -1.24061X_2 -41.98625 X_3 -0.002595X_1X_2+ +0.007725X_1X_3+1.83000 X_2X_3+ 0.000006X^2 +0.402896X^2+ +24.85093X^2

The dispersity is a measurement of the heterogeneity of the particle size in dispersion. It was observed that an increase in the lipid concentration and the concentration of surfactant while keeping the solid lipid: total lipid ratio constant caused a corresponding decrease in PDI and showed a nonlinear relationship in the response surface graph and contour plot. Surfactant plays a major role in the size distribution of particles. The optimum level of surfactant produced a uniform size distribution. Low level of lipid and higher concentrations of surfactant presented higher PDI, which might be due to the higher viscosity of the external phase.

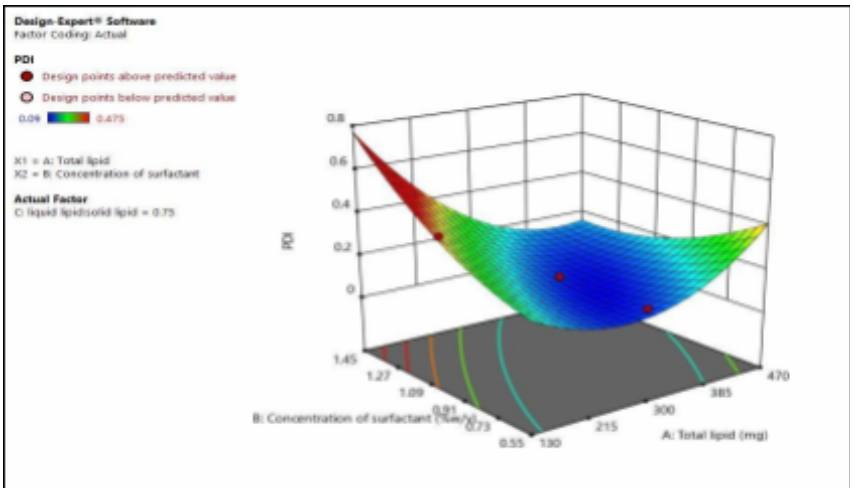

International Journal of Pharmaceutical Research and Applications
Volume 10, Issue 2 Mar–Apr 2025, pp: 1358-1380 www.ijprajournal.com ISSN: 2456-4494

Contour plot of PDI

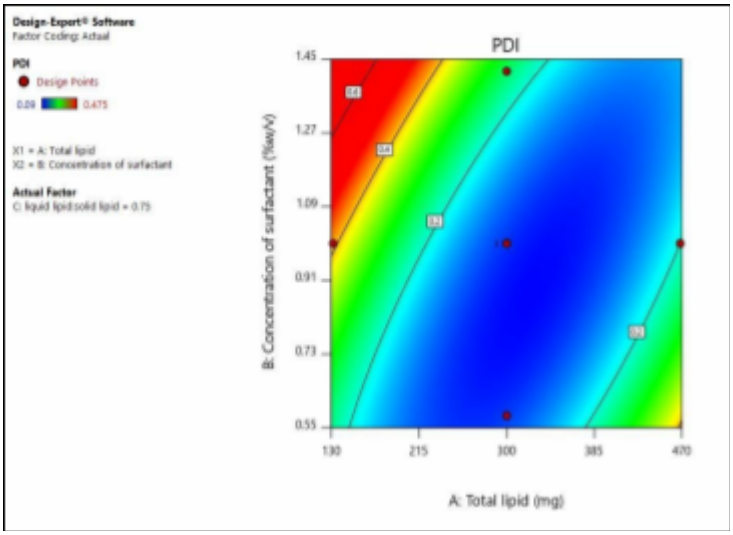

3D surface plot of PDI

Effect of formulation variables on %EE (Y3)

ANOVA table of %Entrapment efficiency

Residual	17.17	13	1.32			
Lack of Fit	15.99	11	1.45	2.46	0.3242	not significant
Pure Error	1.18	2	0.5902			
Cor Total	220.13	16				
Fit statistics						
$_R2$	Adjusted R^2		Predicted R^2		Adeq. Precision	
0.9220	0.9040		0.8882		20.6771	
Source	Sum of	df	Mean square	F-value	p-value	
Model	202.96	3	67.65	51.23	< 0.0001	significant
X_1	160.36	1	160.36	121.43	< 0.0001	Not significant
X_2	39.66	1	39.66	30.03	0.0001	significant
X_3	2.95	1	2.95	2.23	0.1592	significant

The %EE of different batches varied from 67.28 to 80.58% as shown in Table . The effect of selected formulation variables on %EE (Y_3) is presented in Table and the amount of lipid(X_1), and concentration of surfactant (X_2) were found to be significant.

Equation 10 representing the lineal interactions for response Y_3 is: Y_3= 63.95686 +0.034267X_1 - 6.81638X_2 +9.28801X_3 10

As represented in equation 10, the negative effect of the concentration of surfactant X_2 can be attributed to the partition phenomenon. A high level of surfactant facilitates the diffusion of the drug from the internal phase to the external phase. The effect of X_1 and X_2 on %EE while keeping X_3 constant is presented in the response surface graph and the contour plot where the linear relationship is distinct .

International Journal of Pharmaceutical Research and Applications
Volume 10, Issue 2 Mar–Apr 2025, pp: 1358-1380 www.ijprajournal.com ISSN: 2456-4494

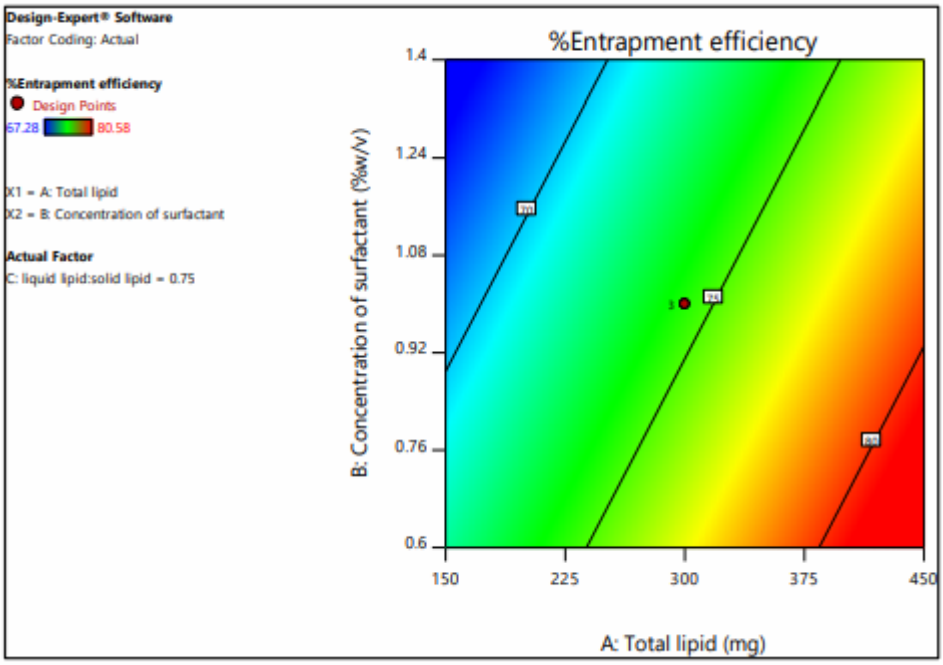

Contour plot of %Entrapment efficiency

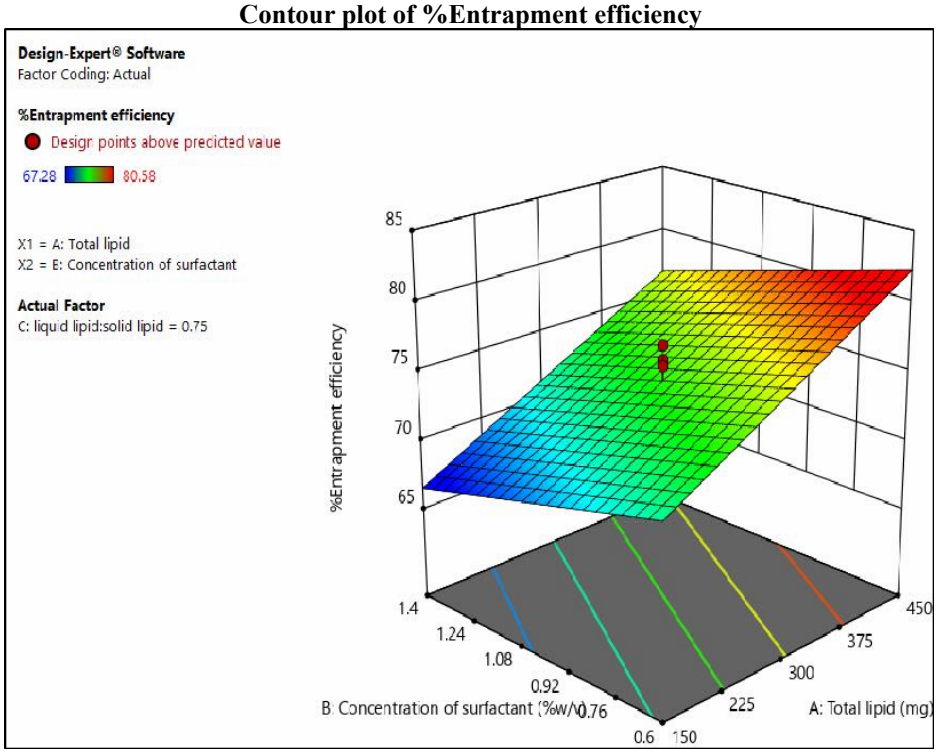

3D surface plot of %Entrapment efficiency

Data optimization and model validation

Graphical method was probed using Design-Expert software to get the optimised formulation. The optimum formulation was built on the defined criteria of %Entrapment efficiency (maximum), particle size (50-150 nm), and PDI (0.1-0.3). Figure represents the overlay plot, indicating the yellow colour region as the design space with the flagged points as the optimum formulation with its composition with the predicted responses. Furthermore, two check point batches were prepared to confirm the validity of the

International Journal of Pharmaceutical Research and Applications
Volume 10, Issue 2 Mar–Apr 2025, pp: 1358-1380 www.ijprajournal.com ISSN: 2456-4494

optimization procedure. It was observed that the experimental values were in the range of the predicted values within 10% of the prediction error. Therefore, the Central composite design for the optimization of VRZ- NLC was validated.

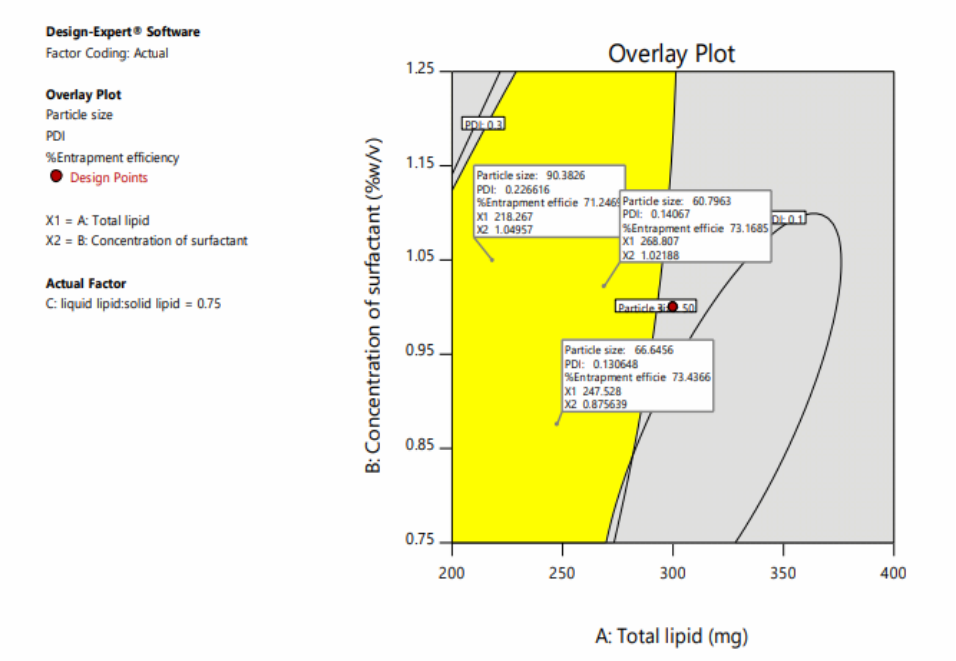

Overlay plot for optimization of VRZ-NLC

Results of validation of optimized model

Checkpoint batches	Optimized batch	Checkpoint batch I	Checkpoint batch II
Total lipid (mg)	247.5	268.8	218.2
Conc. of Surfactant	0.875	1.02	1.04
Solid lipid: Total lipid	0.75	0.75	0.75
R1 (Particle Size nm)			
Predicted value	66.64 nm	60.79 nm	90.38 nm
Measured value	72.58 nm	55.47 nm	84.62 nm
% Predicted error	8.18	-9.59	-6.8
R2 (PDI)			
Predicted value	0.130	0.140	0.226
Measured value	0.137	0.147	0.210
% Predicted error	5.38	4.76	-8.66
R3 (%Entrapment Efficiency)			
Predicted value	73.43	73.16	71.24
Measured value	78.79	78.18	74.89
% Predicted error	6.8	6.42	4.87

International Journal of Pharmaceutical Research and Applications
Volume 10, Issue 2 Mar–Apr 2025, pp: 1358-1380 www.ijprajournal.com ISSN: 2456-4494

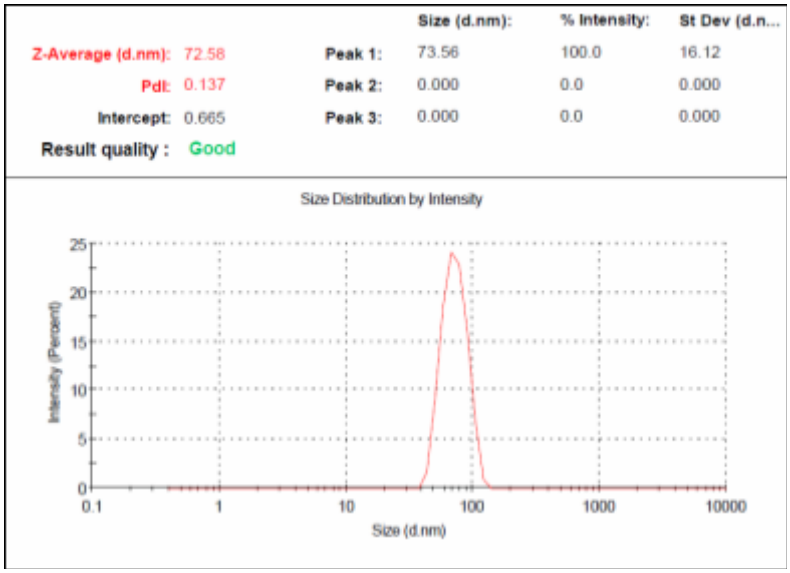

Particle size report of optimised batch of VRZ-NLC

Determination of Zeta potential:

Zeta potential is an important parameter for the stability of any dispersion. Zeta potential for the optimized VRZ-NLC was found to be -9.833± 1.010 mV as shown in figure 23 which indicated that the particles possess sufficient charge to impart repulsion forces for better stability. Poloxamer 188 is a non-ionic stabilizer which provides steric stabilization. Being the melting point of solid lipid higher than liquid lipid, solid lipid recrystallises first entrapping some oil while some oil remaining on surface. The negative zeta potential may be due to the ionization of the non-esterified hydroxyl group present in Capmul MCM

International Journal of Pharmaceutical Research and Applications
Volume 10, Issue 2 Mar–Apr 2025, pp: 1358-1380 www.ijprajournal.com ISSN: 2456-4494

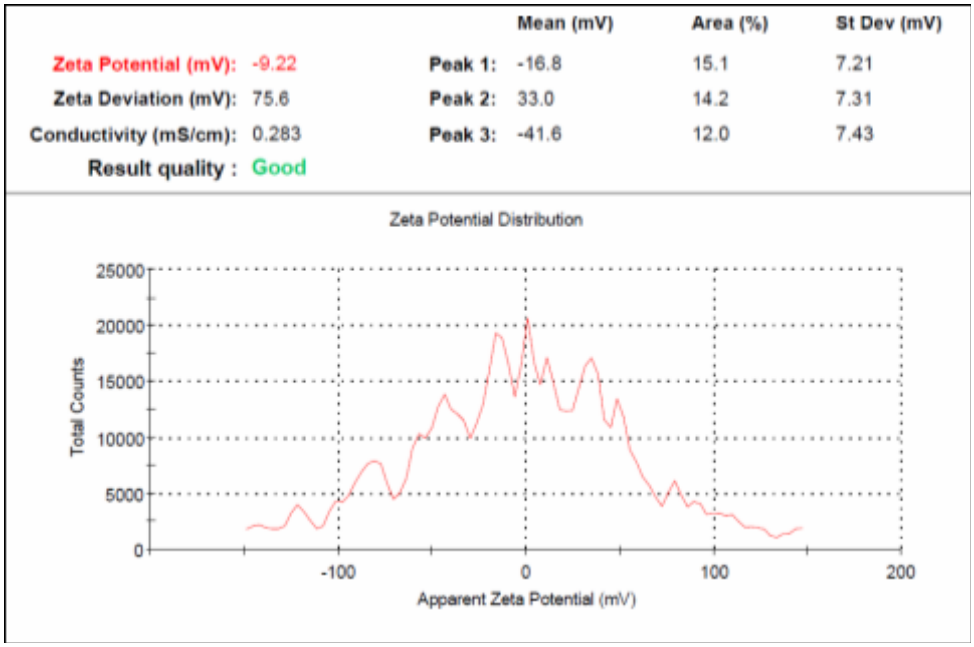

Report of zeta potential

Determination of %Drug loading:

The % Drug loading of the optimized formulation was found to be 6.364 ±0.130%. The drug loading was adequate to carry the required dose of the drug in the lipid matrix.

Transmission electron microscopy

Transmission Electron Microscopy of VRZ-NLC is shown in Figure. The shape of the particles of the lipidic core was nearly spherical and the size of particles was found within nanometer range. The particles did not show a sticking tendency with each other. The particle size obtained from TEM analysis was in line with the particle size measured by dynamic light scattering (DLS). TEM presents the particle size of a single particle while DLS presents the average particle size of dispersion.

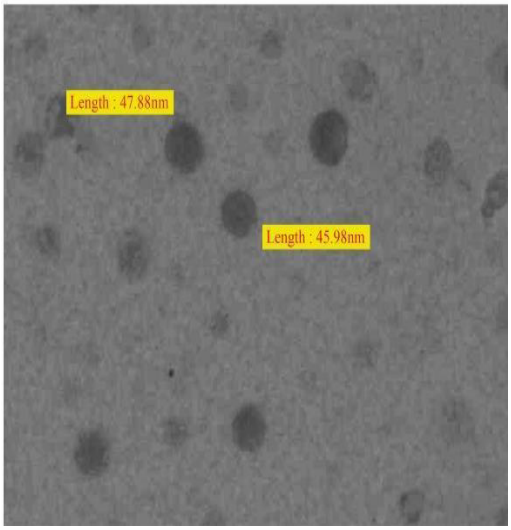

Micrograph of VRZ-NLC by TEM

In vitro drug release study

To predict the release profile upon topical administration, an in vitro release study of VRZ from VRZ-NLCs was performed in STF pH 7.4. From the obtained results, it was apparent that VRZ-NLCs exhibited an initial burst release, i.e., high drug release up to 20.03±0.568% in the first 2 h followed by sustained release up to 91.45±1.299%, till 24 h. Around 15% drug got released in the first 30 min, which can be attributed to the free unentrapped drug present in the dispersion. The drug adsorbed on the outer surface of NLCs, or the drug dissolved in liquid lipid

International Journal of Pharmaceutical Research and Applications
Volume 10, Issue 2 Mar–Apr 2025, pp: 1358-1380 www.ijprajournal.com ISSN: 2456-4494

present on the outer surface of the lipid matrix also caused the burst release, while the drug dissolved within the lipid matrix was released gradually for a longer time leading to a sustained release profile. The solid lipid crystallizes first, entrapping some drug and making a matrix while the liquid lipid remains on the surface. The drug dissolved in liquid lipid contributes towards burst release.

The release data were analysed by using different mathematical models, i.e., zero order, first order, Higuchi, and Korsmeyer–Peppas model by plotting the cumulative percent drug release versus time, log cumulative percent drug remaining versus time, cumulative percent drug release versus the square root of time and log cumulative percent drug release versus log time respectively, to define the release kinetics. The Regression co-efficient for zero-order, first-order and Higuchi model were found to be 0.944, 0.9846 and 0.986 respectively. Release from NLCs fitted Higuchi model better than other models (R^2=0.986) and was found to be diffusion controlled from a homogeneous and granular matrix system. The drug release from a matrix system is said to follow Higuchi's release kinetics if the amount of drug released is directly proportional to the square root of time. The value of diffusion exponent "n" obtained from the Korsmeyer-Peppas equation was found to be 0.5 indicating that the release was by Fickian diffusion.

Preparation of Chitosan coated NLC(VRZ-CH-NLC):

The results of chitosan coating process are summarized in table. The chitosan hydrochloride solution ranging from 0.2%w/v to 1%w/v were added to the VRZ-NLC dispersion. The solution containing 0.2%w/v Chitosan hydrochloride in proportion of 3:1 and 2:1 (VRZ-NLC: Chitosan hydrochloride solution) could not produce positively charged NLC. This might be related to inadequate amount of positively charged chitosan molecules for complete coating of negatively charged NLC while it produced aggregation in proportion of 1:1. Similarly, 1% w/v Chitosan hydrochloride solution in proportion of 10:1 (NLC: Chitosan hydrochloride solution) produced aggregation. 0.5%w/v Chitosan hydrochloride solution in ratio of 2.5:1(VRZ-NLC: Chitosan hydrochloride solution) could yield positively charged NLC with zeta potential of 16.866±1.36 mV because of sufficient availability of Chitosan molecules which could provide adequate coating on the particles. The zeta potential report is shown in figure.

International Journal of Pharmaceutical Research and Applications
Volume 10, Issue 2 Mar–Apr 2025, pp: 1358-1380 www.ijprajournal.com ISSN: 2456-4494

Results of preparation of VRZ-CH-NLC

Sr No	Chitosan HCl %w/v	Dilution ratio (NLC: Chitosan HCl)	Observation
1	0.2	-	20.866±1.05 mV
2	0.2	40:1	-4.79±0.492 mV
3	0.2	3:1	-2.796 ± 1.00mV
4	0.2	2:1	-1.47±0.439 mV
5	0.2	1:1	Aggregation
6	1	10:1	Aggregation
7	0.5	10:1	Aggregation
8	0.5	2.5:1	16.866±1.36 mV

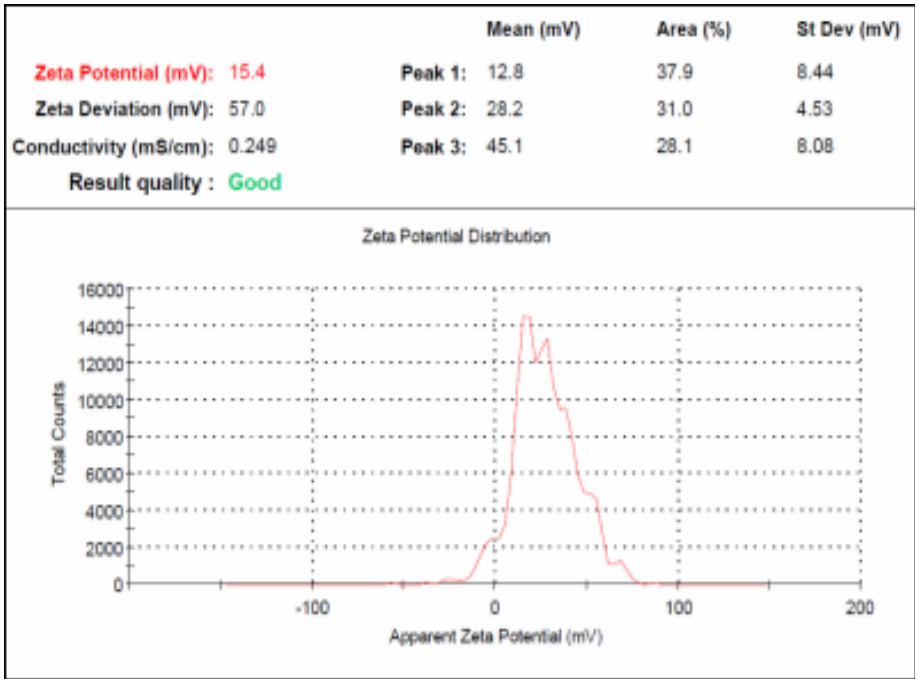

Zeta potential report of optimized VRZ-CH-NLC

Evaluation of Chitosan coated NLC(VRZ-CH-NLC):

Particle Size and PDI

Particle size and Particle size distribution was determined using Dynamic light scattering. Particle size was found to be 114.16±7.919 nm and PDI was found to be 0.125±0.014. The size distribution report is shown in Figure. An increase in particle size as compared to naked NLC can be ascribed to the coating of the particles with the mucoadhesive polymer.

International Journal of Pharmaceutical Research and Applications
Volume 10, Issue 2 Mar–Apr 2025, pp: 1358-1380 www.ijprajournal.com ISSN: 2456-4494

			Size (d.nm):	% Intensity:	St Dev (d.n...
Z-Average (d.nm):	111.8	Peak 1:	120.5	100.0	22.42
PdI:	0.123	Peak 2:	0.000	0.0	0.000
Intercept:	0.688	Peak 3:	0.000	0.0	0.000
Result quality :	Good				

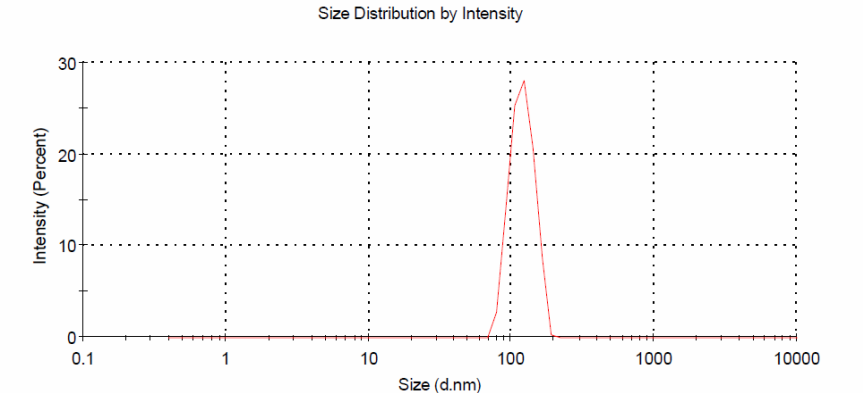

Particle size report of VRZ-CH-NLC

%Entrapment efficiency and %Drug loading:

The %entrapment efficiency and %Drug loading were found to be 77.94±1.929 % and 6.302±0.142 % respectively. There isn't significant difference in the %Entrapment efficiency of coated and uncoated NLC which ascertain that NLC remain intact and are not disrupted during coating process.

Transmission Electron Microscopy (TEM) of core shell Nanoparticles

Transmission Electron Microscopy of the VRZ-CH-NLC is shown Figure. The particles were in spherical morphology and the coating around the particles is evidently seen. The increase in particle size due to coating of Chitosan on surface of NLC is in agreement with the results obtained from particle size analysis by Zetasizer.

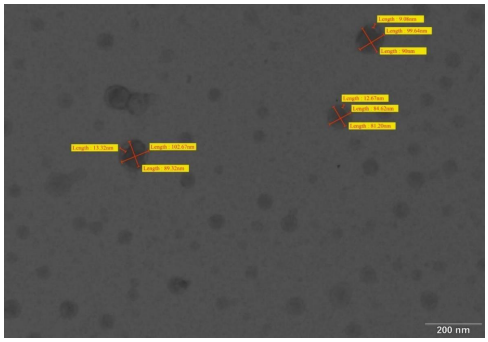

Micrograph of VRZ-CH-NLC by TEM

In vitro drug release study:

The in vitro release profile of VRZ-CH-NLC is shown in figure and is compared with VRZ-NLC and VRZ-suspension. From the obtained results, it was evident that VRZ-CH-NLCs demonstrated an initial burst release, i.e., up to 15% drug release in the first 30 min. But the drug release slowed down later producing sustained release pattern releasing drug up to 75.54±2.710%, till 24 hr. The initial burst release can be related to the free unentrapped drug present in the dispersion while the drug release from the NLC core got prolonged because of the surface coating with mucoadhesive polymer. Before getting released into the medium, VRZ had to go through thenanostructure core and adhesive and gel like microenvironment of coating which obviously slowed down the drug release rate from VRZ-CH-NLC.

The release data were fitted in different mathematical models, i.e., zero order, first order, Higuchi, and Korsmeyer–Peppas model. The Regression co-efficient for zero- order, first-order and Higuchi model were found to be 0.9566, 0.9859 and 0.9863 respectively. Release from NLCs fitted Higuchi model better than other models (R^2=0.9863) and was found to be diffusion controlled from a homogeneous and granular matrix system. The drug release from a matrix system is said to follow Higuchi's release kinetics if the amount of drug released is directly proportional to the square root of time. The value of diffusion exponent "n" obtained from the

International Journal of Pharmaceutical Research and Applications
Volume 10, Issue 2 Mar–Apr 2025, pp: 1358-1380 www.ijprajournal.com ISSN: 2456-4494

Korsmeyer-Peppas equation was found to be 0.448 indicating that the release was by Fickian diffusion. So, it was inferred that the surface coating doesn't alter the kinetics of drug release from lipid matrix.

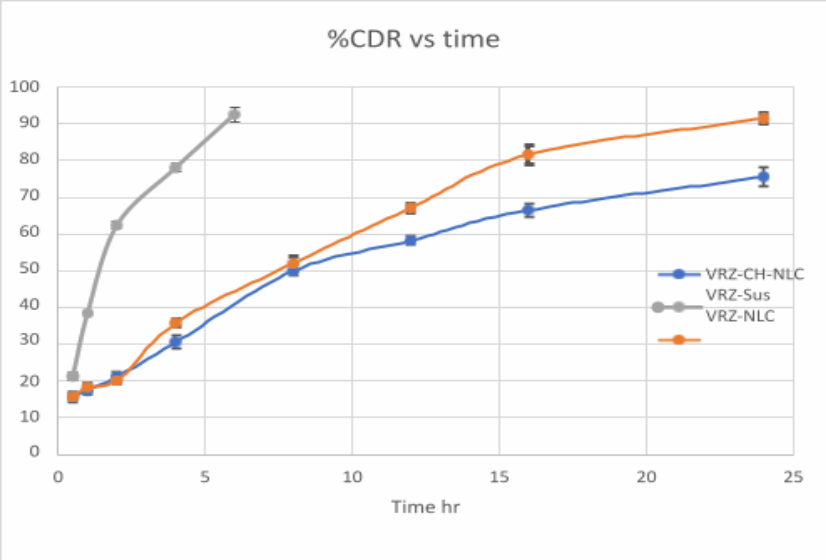

In vitro drug release profile of VRZ-CH-NLC, VRZ-NLC, VRZ-SUS

pH and isotonicity:

The pH of optimized VRZ-CH-NLC measured using calibrated pH meter at 25 ^{0} C was found to be 6.8 ± 0.1. Isotonicity of VRZ-CH-NLC was evaluated by haemolytic method. The shape and size of RBCs were not altered when exposed to VRZ-CH-NLC and found to be very similar to the RBCs treated with normal saline solution which indicated that the formulation was isotonic with lachrymal fluid and blood.

Sterilization and Sterility testing

The sterilization of the optimized VRZ-CH-NLC was carried out successfully using membrane filtration technique aseptically. The sterile samples were subjected to sterility testing by direct inoculation method as per IP 2010. No growth was observed in soyabean casein and fluid thioglycolate media after incubation period of 14 days hence they passed sterility testing.

Stability study

The developed VRZ-CH-NLC formulation was found to be stable for 6 months at 5±3°C and 30 ± 2°C/65 ± 5% RH. No significant change in the physical appearance average particle size, PDI, zeta potential and %EE were noted during the stability studies. Hence it can be concluded that Voriconazole loaded surface coated lipidic nanoparticles were stable at 5±3°C as well as 30 ± 2°C/65 ± 5% RH for 6 months.

International Journal of Pharmaceutical Research and Applications
Volume 10, Issue 2 Mar–Apr 2025, pp: 1358-1380 www.ijprajournal.com ISSN: 2456-4494

Stability studies data for VRZ-CH-NLC at 30 ° C ± 2 ° C / 65% ± 5% RH

Time(months)	Particle size (nm)	PDI	Zeta potential mV	% EE
0	114.16±7.919	0.125±0.014	16.866±1.36	77.94±1.93
0.5	118.5667±4.743	0.128±0.0141	15.967±0.76	77.703±1.92
1	122.6±2.458	0.129±0.0114	15.500±0.67	77.523±1.55
2	127.0333±2.546	0.132±0.0114	14.933±0.62	77.373±1.52
3	129.3667±2.322	0.135±0.0114	14.500±0.71	77.207±1.56
4	132.1333±2.11	0.136±0.0118	14.100±0.50	76.910±1.66
5	136.3333±1.329	0.138±0.0118	13.667±0.45	76.637±1.64
6	141.6333±2.315	0.140±0.0130	12.950±1.15	76.403±1.58

Stability studies data for VRZ-CH-NLC at 5⁰ C ± 3 ° C

Time months	Particle size nm	PDI	Zeta potential mV	% EE
0	114.16±7.919	0.125±0.014	16.867±1.361	77.94±1.929
0.5	117.6±6.555	0.129±0.014	16.433±0.971	77.817±1.929
1	121.1333±3.566	0.135±0.012	15.933±0.660	77.677±1.649
2	123.7±2.987	0.138±0.011	15.400±0.779	77.610±1.633
3	124.0333±2.792	0.143±0.011	14.900±0.726	77.407±1.620
4	125.7667±1.81	0.150±0.0087	14.467±0.602	77.280±1.641
5	129±2.698	0.154±0.0057	14.200±0.497	76.960±1.521
6	130.7333±2.747	0.162±0.0065	13.367±1.066	76.770±1.558

V.

VI. CONCLUSION

Ocular diseases and visual impairment are highly widespread worldwide and can be enervating to the affected patient. Topical application is one of the most used routes of administration for treating ophthalmic conditions due to patient compliance and ease of manufacturing. Nearly 90% of the ophthalmic formulations now on the market are in conventional topical dosage forms such solutions, suspensions, and ointments. However, topical administration presents various challenges such as less capacity of cul-de-sac, movement of lower eyelid, biphasic environment of cornea, abundant blood and lymphatic supply to conjunctiva, tear film and continuous tear turnover, presence of mucin in tear film, reflex blinking and nasolacrimal drainage, blood-aqueous barrier, blood-retinal barrier, presence metabolic enzymes and efflux pumps yielding bioavailability in the range of of 1–5% of the total administered dose.

Fungal keratitis is an inflammation of the layers of the cornea mainly caused by fungi such as Aspergillus spp., Fusarium spp. or yeast-like Candida albicans. Although, it can be occurred due to many other species. In fungal keratitis, early diagnosis, and proper selection of the antimycotic agents play a crucial role. If it is not treated, it can lead to blindness. Natamycin and Amphotericin B have been used for fungal keratitis, but azoles have been used widely due to their greater spectra. Voriconazole (VRZ), a synthetic triazole, is a broad-spectrum antifungal agent that is particularly effective against Aspergillus spp., Candida spp., Fusarium spp., and Scedosporium spp. It has also shown effectiveness against resistant infection to other first-line azoles. Chitosan coated lipidic particles containing Voriconazole were formulated to address its limited solubility and permeability and to prolong its residence time.

QbD based approach was adopted for systematic development of the formulation. The VRZ-NLC formulation containing Stearic acid, Capmul MCM, Poloxamer 188 with high solubilization for Voriconazole was successfully developed using High speed homogenizer. The formulation was optimized using Central composite design using Design Expert. The nanoparticle formulation was characterized for particle size, PDI, Zeta-potential, %EE, %DL, TEM, and ex vivo

International Journal of Pharmaceutical Research and Applications
Volume 10, Issue 2 Mar–Apr 2025, pp: 1358-1380 www.ijprajournal.com ISSN: 2456-4494

permeation. In vitro drug release studies revealed sustained release profile. VRZ-NLC were coated with Chitosan Hydrochloride solution to produce Voriconazole containing chitosan coated NLC. VRZ-CH-NLC possessed positive charge 16.866±1.36 mV which can contribute to the electrostatic interaction. The particle size was found to be 114.16±7.919 with PDI 0.125±0.014. They offered good %entrapment efficiency and %drug loading 77.94±1.929 % and 6.302±0.142 % respectively. TEM micrograph clearly indicated coating on NLC surface. VRZ-CH-NLC presented initial burst release followed by sustained release with fickian diffusion for 24 hrs in in vitro drug release study.

REFERENCES:

[1]. Schuster AK, Erb C, Hoffmann EM, Dietlein T, Pfeiffer N. The Diagnosis and Treatment of Glaucoma. Dtsch Arztebl Int. 2020;117:225–34.

[2]. Chen H, Chen H. Recent developments in ocular drug delivery Recent developments in ocular drug delivery. J Drug Target. 2015;2330(October):597– 604.

[3]. Mandpe L, Pokharkar V. Quality by design approach to understand the process of optimization of iloperidone nanostructured lipid carriers for oral bioavailability enhancement. Pharm Dev Technol [Internet]. 2015 Apr 3;20(3):320–9. Available from: https://doi.org/10.3109/10837450.2013.867445

[4]. Jojo GM, Kuppusamy G, De A, Karri VVSNR. Formulation and optimization of intranasal nanolipid carriers of pioglitazone for the repurposing in Alzheimer's disease using Box-Behnken design. Drug Dev Ind Pharm. 2019 Jul 3;45(7):1061–72.

[5]. Gurumukhi VC, Bari SB. Fabrication of efavirenz loaded nano-formulation using quality by design (QbD) based approach : Exploring characterizations and in vivo safety. J Drug Deliv Sci Technol [Internet]. 2020;56(January):101545. Available from: https://doi.org/10.1016/j.jddst.2020.101545

[6]. Ferreira M, Chaves LL, Costa A, Reis S. Optimization of nanostructured lipid carriers loaded with methotrexate : A tool for in fl ammatory and cancer therapy. Int J Pharm. 2015;492:65–72.

[7]. Abdelbary G, Fahmy RH. Diazepam-Loaded Solid Lipid Nanoparticles: Design and Characterization. AAPS PharmSciTech [Internet]. 2009;10(1):211–9. Available from: https://doi.org/10.1208/s12249-009-9197-2

[8]. "Shaal LA and MRH and KCM and KCM". Preserving hesperetin nanosuspensions for dermal application. "Die Pharmazie - An International Journal of Pharmaceutical Sciences" [Internet]. 2010;65:86–92. Available from: https://www.ingentaconnect.com/content/govi/pharmaz/2010/00000065/00000002/art00003

[9]. Bajaj A, Rao MRP, Pardeshi A, Sali D. Nanocrystallization by Evaporative Antisolvent Technique for Solubility and Bioavailability Enhancement of Telmisartan. AAPS PharmSciTech. 2012;13(4):1331–40.

[10]. Patel, Akanksha and Dharamsi A. Nanocrystals- A Substantial Platform for Drug Delivery Applications. Current Nanomedicine(Formerly: Recent Patents on Nanomedicine) [Internet]. 2021;11(4):202–12. Available from: https://www.ingentaconnect.com/content/ben/cnanom/2021/00000011/00000004/art00003

[11]. Ling Tan JS, Roberts CJ, Billa N. Mucoadhesive chitosan-coated nanostructured lipid carriers for oral delivery of amphotericin B. Pharm Dev Technol [Internet]. 2019 Apr 21;24(4):504–12. Available from: https://doi.org/10.1080/10837450.2018.1515225

[12]. Zhang W, Li X, Ye T, Chen F, Sun X, Kong J, et al. Design , characterization , and in vitro cellular inhibition and uptake of optimized genistein-loaded NLC for the prevention of posterior capsular opacification using response surface methodology. Int J Pharm [Internet]. 2013;454(1):354–66. Available from: http://dx.doi.org/10.1016/j.ijpharm.2013.07.032

[13]. Burhan AM, Klahan B, Cummins W, Andr V, Byrne ME, Reilly NJO, et al.

International Journal of Pharmaceutical Research and Applications
Volume 10, Issue 2 Mar–Apr 2025, pp: 1358-1380 www.ijprajournal.com ISSN: 2456-4494

Posterior Segment Ophthalmic Drug Delivery : Role of Muco-Adhesion with a Special Focus on Chitosan. Pharmaceutics. 2021;(13):1685.

[14]. Li J, Liu D, Tan G, Zhao Z, Yang X, Pan W. A comparative study on the efficiency of chitosan-N-acetylcysteine, chitosan oligosaccharides or carboxymethyl chitosan surface modified nanostructured lipid carrier for ophthalmic delivery of curcumin. Carbohydr Polym. 2016;146:435–444.

[15]. Lakhani P, Patil A, Wu K wei, Sweeney C, Tripathi S, Avula B, et al. Optimization, stabilization, and characterization of amphotericin B loaded nanostructured lipid carriers for ocular drug delivery. Int J Pharm [Internet]. 2019;118771. Available from: https://doi.org/10.1016/j.ijpharm.2019.118771

[16]. Thapa C, Ahad A, Aqil Mohd, Imam SS, Sultana Y. Formulation and optimization of nanostructured lipid carriers to enhance oral bioavailability of telmisartan using Box–Behnken design. J Drug Deliv Sci Technol. 2018 Apr;44:431–9.

[17]. Soni K, Rizwanullah Md, Kohli K. Development and optimization of sulforaphane-loaded nanostructured lipid carriers by the Box-Behnken design for improved oral efficacy against cancer: in vitro, ex vivo and in vivo assessments. Artif Cells Nanomed Biotechnol. 2018 Oct 31;46(sup1):15–31.

[18]. Ebrahimi HA, Javadzadeh Y, Hamidi M, Jalali MB. Repaglinide-loaded solid lipid nanoparticles: effect of using different surfactants/stabilizers on physicochemical properties of nanoparticles. DARU Journal of Pharmaceutical Sciences. 2015 Dec 21;23(1):46.

[19]. Tan SW, Billa N, Roberts CR, Burley JC. Surfactant effects on the physical characteristics of Amphotericin B-containing nanostructured lipid carriers. Colloids Surf A Physicochem Eng Asp. 2010 Dec;372(1–3):73–9.

[20]. Han F, Li S, Yin R, Liu H, Xu L. Effect of surfactants on the formation and characterization of a new type of colloidal drug delivery system: Nanostructured lipid carriers. Colloids Surf A Physicochem Eng Asp. 2008 Feb;315(1–3):210– 6.

[21]. Shekhawat P, Pokharkar V. Risk assessment and QbD based optimization of an Eprosartan mesylate nanosuspension: In-vitro characterization, PAMPA and in- vivo assessment. Int J Pharm. 2019 Aug;567:118415.

[22]. Patel A, Dharamsi A. Nanocrystals- A Substantial Platform for Drug Delivery Applications. Current Nanomedicine. 2021;11:202–12.

[23]. Alshweiat A, Csóka IiI, Tömösi F, Janáky T, Kovács A, Gáspár R, et al. Nasal delivery of nanosuspension-based mucoadhesive formulation with improved bioavailability of loratadine: Preparation, characterization, and in vivo evaluation. Int J Pharm [Internet]. 2020;579:119166. Available from: https://doi.org/10.1016/j.ijpharm.2020.119166

[24]. Padmaa Paarakh M, Ani Jose P, Setty CM, Christoper GVP. Release Kinetics- Concepts and Applications. International Journal of Pharmacy Research & Technology. 2018;8:12–20.

[25]. Sandri G, Motta S, Bonferoni MC, Brocca P, Rossi S, Ferrari F, et al. Chitosan- coupled Solid Lipid Nanoparticles : tuning nanostructure and mucoadhesion.European Journal of Pharmaceutics and Biophar. [Internet]. 2016; 110:13–8. Available from: http://dx.doi.org/10.1016/j.ejpb.2016.10.010

[26]. Kalam MA. The potential application of hyaluronic acid coated chitosan nanoparticles in ocular delivery of dexamethasone. Int J Biol Macromol [Internet].2016; Available from: http://dx.doi.org/10.1016/j.ijbiomac.2016.05.016

[27]. Fu T, Yi J, Lv S, Zhang B. Ocular amphotericin B delivery by chitosan modified nanostructured lipid carriers for fungal keratitis targeted therapy. J Liposome Res. 2017;27(3):228–33.

[28]. Li J, Jin X, Zhang L, Yang Y, Liu R, Li Z. Comparison of Different Chitosan Lipid Nanoparticles for Improved Ophthalmic Tetrandrine Delivery: Formulation , Characterization , Pharmacokinetic and Molecular Dynamics

Simulation. J Pharm Sci [Internet]. 2020;1–11. Available from: https://doi.org/10.1016/j.xphs.2020.09.010

[29]. Dubey V, Mohan P, Dangi JS, Kesavan K. Brinzolamide Loaded Chitosan-Pectin Mucoadhesive Nanocapsules for Management of Glaucoma: Formulation, Characterization and Pharmacodynamic Study. International Journal of Biological Macromolecules [Internet]. 2019;152(June 2020):1224–32. Available from: https://doi.org/10.1016/j.ijbiomac.2019.10.219